What Limits Zonal Flow Shears in (nearly) Collisionless Drift-Wave Turbulence?

T. Zhang[1], P.H. Diamond[1], and R.A. Heinonen[1,2]
Department of Physics, UCSD[1] and University of Rome, Italy[2]
Supported by US D.O.E under Grant No. DE-FG02-04ER54738

*Note that bracketed numbers, like [1], indicate sources, which will be shown at the end

APS DPP 2021

UC San Diego

Introduction

- Drift wave - zonal flow turbulence is self-regulating and frequently thought of as a predator-prey system [6]
- Zonal shear feedback on the prey (drift wave) is central to transport regulation
- Predator-prey model between zonal flows and drift waves: [3, 4, 10]:

$$\partial_t N = \gamma N - \alpha E_V N - \Delta\omega N^2$$

$$\partial_t E_V = \alpha N E_V - \nu_F E_V - \gamma_{nl}(N, E_V) E_V * E_V$$

- With $\gamma_{nl} = 0$, two fixed points appear:

No Flow: $E_V = 0$ and $N = \frac{\gamma}{\Delta\omega}$ Flow: $E_V = \frac{\alpha\gamma - \Delta\omega\nu_F}{\alpha^2}$ and $N = \frac{\nu_F}{\alpha}$

- $\nu_F \to 0$ is akin to a Dimits Shift Regime ($E_{ZonalFlow} >> E_{DriftWave}$)
- Identifies the problem of collisionless saturation → what else limits E_{ZF} ?
- Tertiary instabilities like K-H → zonal flow instability?!

Critical Questions

- In what way does the stability criterion dictate zonal flow stability and what is the impact of zonal flow instability on DW-ZF turbulence?
- Does gradient of the mean potential vorticity ($\nabla\langle PV\rangle = \nabla(\langle n\rangle - \langle\nabla_\perp^2\phi\rangle)$) indicate zonal flow instability?
- How does the profile of the potential vorticity correlate with saturated turbulence levels?
- How does zonal flow marginality correlate with turbulence levels and what are the implications?
- Does R = $\frac{E_{ZonalFlow}}{E_{DriftWave}}$ show a correlation with the profile of mean potential vorticity (PV) and zonal flow stability?

Notation

- $n = \widetilde{n} + \langle n \rangle$ with $\widetilde{n}$ = density fluctuation and $\langle n \rangle$ = zonally averaged density
- $\langle n \rangle = n_z + n_0$ with n_z = fluctuation in zonally averaged density and n_0 = background density $= \kappa * x$
- $\phi = \widetilde{\phi} + \langle \phi \rangle$
- $\nabla \langle PV \rangle = \partial_x (\langle n \rangle - \nabla^2 \langle \phi \rangle)$

Hasegawa-Wakatani Model

$$\partial_t \nabla_\perp^2 \phi + \{\phi, \nabla_\perp^2 \phi\} = \alpha(\phi - n) - \mu \nabla_\perp^2 \phi - \nu \nabla_\perp^6 \phi \rightarrow \partial_t \langle \nabla_\perp^2 \phi \rangle - \partial_x \langle (\nabla_\perp^2 \phi \partial_y \phi) \rangle = -\mu \langle \nabla_\perp^2 \phi \rangle \text{ [1,9]}$$

$$\partial_t n + \{\phi, n\} = \alpha(\phi - n) - \kappa \partial_y \phi - D \nabla_\perp^4 n \rightarrow \partial_t \langle n \rangle - \partial_x \langle (n \partial_y \phi) \rangle = -D \langle \nabla_\perp^4 n \rangle$$

$\alpha_{eff} = \frac{\alpha}{\kappa}$ μ - flow-damping parameter κ - linear density gradient drive

- R = $\frac{E_{ZF}}{E_{DW}}$ calculated in a 10 x 5 region selected from the simulation space
- Zonal Flow Energy = $E_{ZF} = \int \int |\langle \nabla_\perp \phi \rangle|^2 dxdy$ for $\alpha_{eff} > 1$
- Drift Wave Energy = $E_{DW} = \int \int |\tilde{n}|^2 + |\nabla_\perp \tilde{\phi}|^2 dxdy \simeq \int \int |\tilde{\phi}|^2 + |\nabla_\perp \tilde{\phi}|^2 dxdy$ for $\alpha_{eff} > 1$

Zonal Instability Criterion

Inviscid, Incompressible 2D Fluid	Hasegawa-Mima ($\alpha_{eff} > 1$)
Rayleigh Criterion	Rayleigh-Kuo Criterion
Necessary condition that states $\nabla(\nabla^2\phi) = 0$ for shear flow instability to occur	Necessary condition that states $\nabla(\langle n \rangle - \nabla^2\langle\phi\rangle) = 0$ for shear flow instability to occur

Both are generalized inflection point theorems

Procedure For R vs. ∇<PV>

- Main Question: Does $\nabla(\langle PV \rangle)$ have any observable effect on R $= \frac{E_{ZF}}{E_{DW}}$?
- Produced BOUT++ simulations with varied density gradient drive $[\kappa]$ (1 to 1.75) and flow damping $[\mu]$ (0.01 to 0.2)
- R calculated through integrating over a 10 x 5 region shown in Figure 1
  - Other region sizes (5x5, 7x7, 9x9) gave similar results
- Points are arbitrary selected to ensure impartial analysis of simulation space
  - Points near simulation border removed, as border cells are constrained by boundary conditions
- Gauged effects of altering κ and μ on $\nabla\langle PV \rangle$

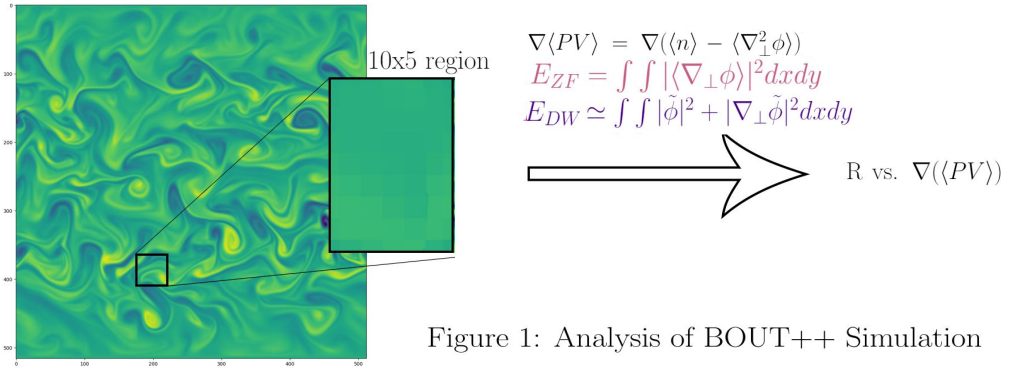

Figure 1: Analysis of BOUT++ Simulation

Results I - “The Big Picture Plot I”

- Variance in R $= \frac{E_{ZF}}{E_{DW}}$ and $\nabla(\langle PV \rangle)$ larger for lower μ
  - Less restriction on flow configuration
- Maximum value for R decreases as μ increases as expected
- For areas with $R < 1$, centralization occurs around $\nabla\langle PV \rangle = 1.5$

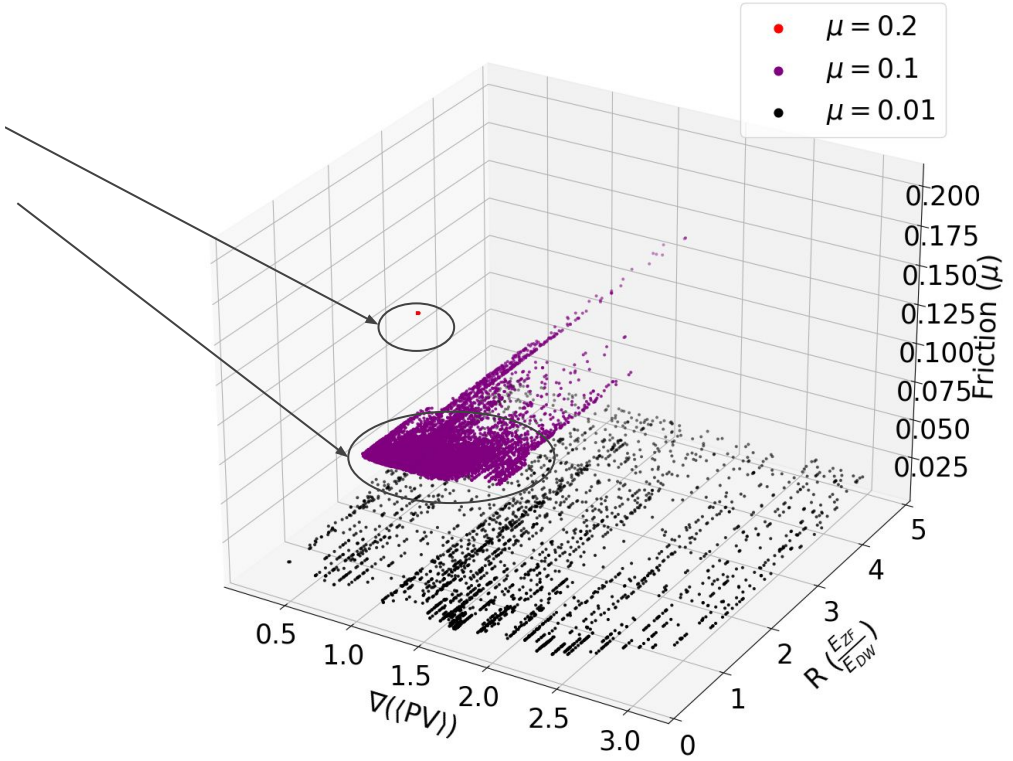

Figure 2: 3D Plot of R vs. $\nabla(\langle PV \rangle)$ vs. μ

Results II - Comparison Between Larger and Lower Damping

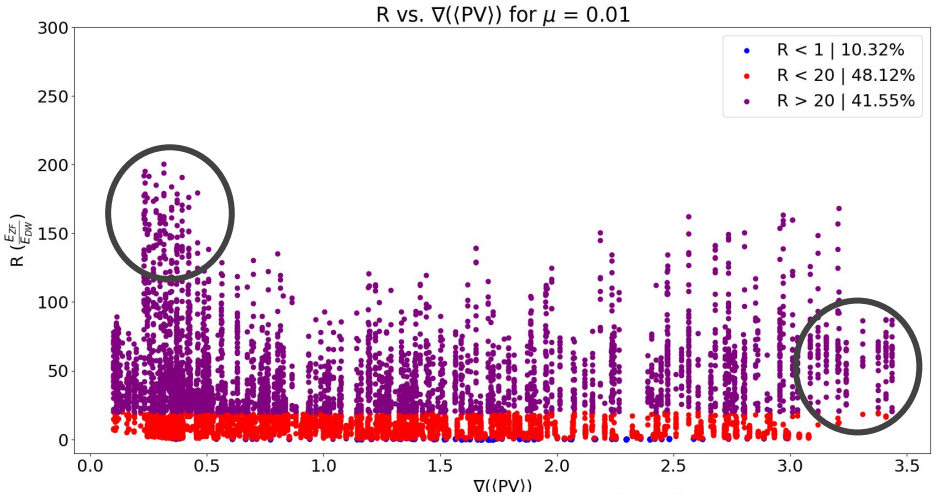

Figure 3: Distribution of R vs. $\nabla\langle PV\rangle$ for $\mu = 0.01$

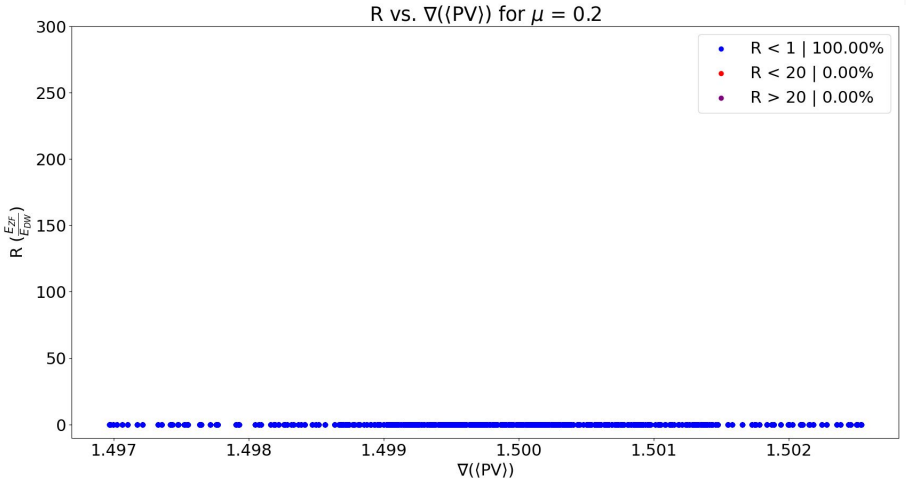

Figure 4: Distribution of R vs. $\nabla\langle PV\rangle$ for $\mu = 0.2$

- More zonal flow energy evident in lower damping conditions
- Dimits-like region visible in lower damping circled in black, disappears with higher damping
- For areas with $R < 1$, both damping scenarios show centralization around $\nabla\langle PV\rangle = 1.5$
- Most locations with low R values have $\nabla\langle PV\rangle \neq 0$, suggests RK stability isn't major player

Results III - ∇<PV> Profile Dependence on Frictional Damping

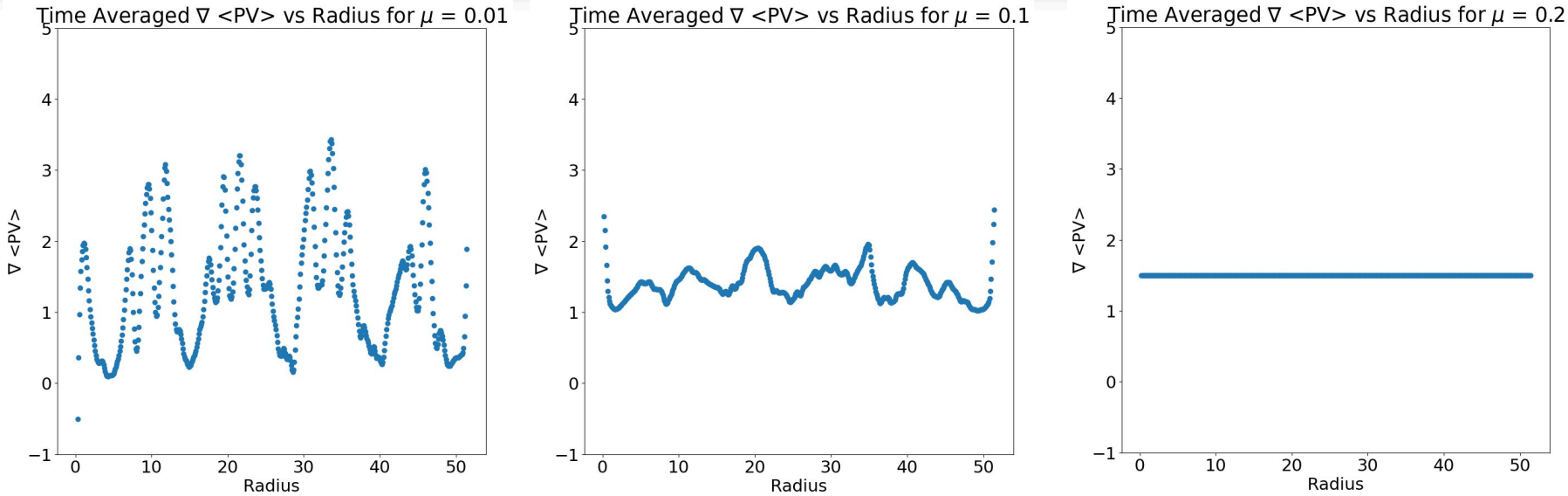

Figure 6: $\nabla\langle PV\rangle$ profiles with increasing μ

- Graphs shown here have $\alpha_{eff} = 2$, $\kappa = 1.5$
- Variance in $\nabla\langle PV\rangle$ decreases as μ increases
- Most common value of $\nabla\langle PV\rangle$ stays around $\nabla\langle PV\rangle = 1.5$

Results IV - “The Big Picture Plot II”

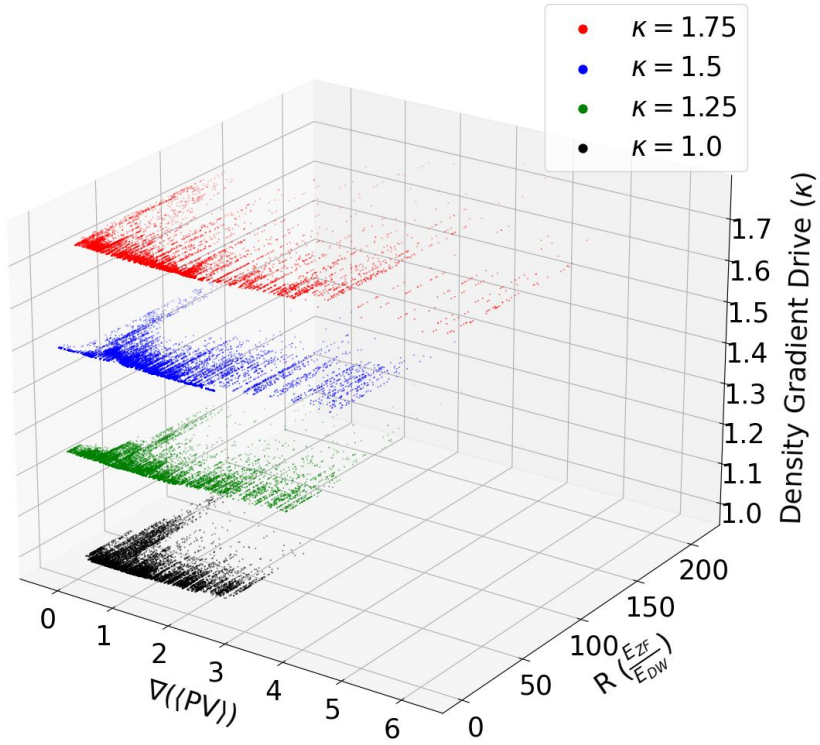

Figure 7: 3D Plot of R vs. $\nabla\langle PV\rangle$ vs. κ

- Keeping α_{eff} constant, R vs. $\nabla\langle PV\rangle$ graphs have similar shape independent of κ
- Larger value of κ translates the graph positively along the $\nabla\langle PV\rangle$ axis
- Stronger background gradient also produces a wider range of $\nabla\langle PV\rangle$

Results V - Comparison Between Higher and Lower Density Gradient Drive

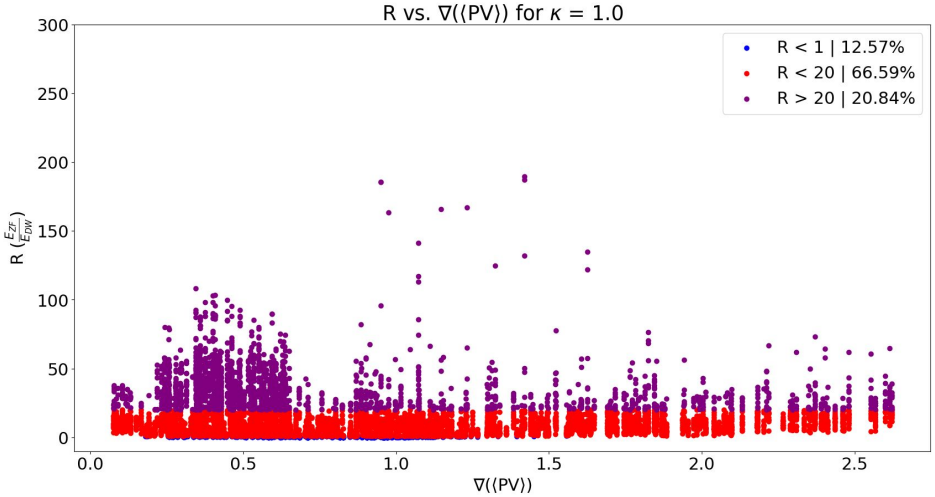

Figure 8: Distribution of R vs. $\nabla\langle PV\rangle$ for $\kappa = 1.0$

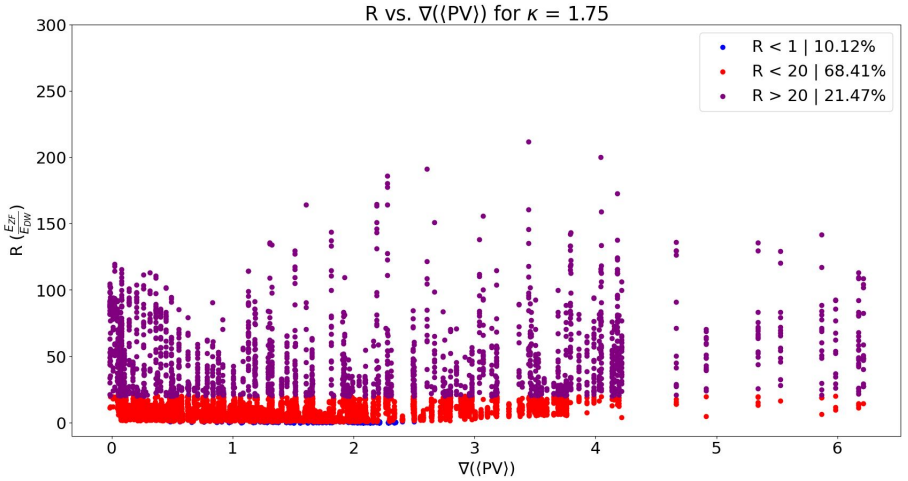

Figure 9: Distribution of R vs. $\nabla\langle PV\rangle$ for $\kappa = 1.75$

- Dimits-like regime are apparent, with two tails appearing with $R > 20$
- Increasing κ doesn't diminish the size or volume of these tails

Results VI - ∇<PV> Profile Dependence on Density Gradient Drive

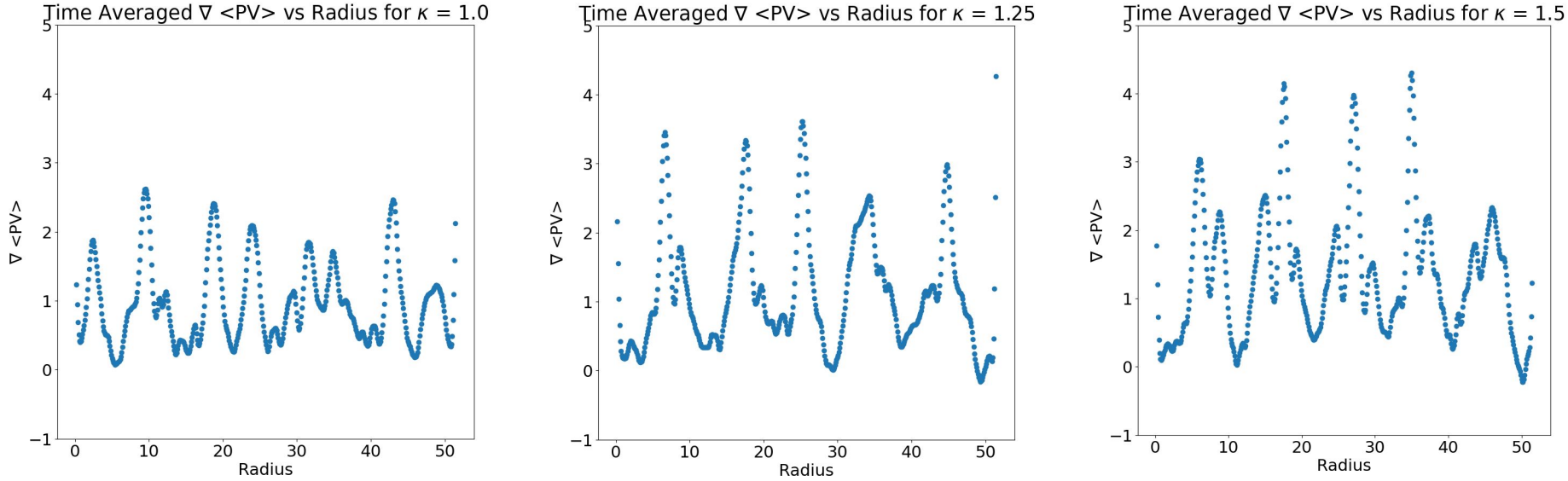

Figure 10: $\nabla\langle PV\rangle$ profiles with increasing κ

- Graphs shown here have $\alpha_{eff} = 2$, $\mu = 0.01$
- Most common value of $\nabla\langle PV\rangle$ increases as κ increases
- Larger κ still have several areas with $\nabla\langle PV\rangle = 0$

Key Results

- R ($\frac{E_{ZF}}{E_{DW}}$) isn't correlated with the RK criterion ($\nabla\langle PV\rangle = 0$)
- Persistent Dimits-like regimes present in low friction damping scenarios and independent of kappa
- With α_{eff} constant, increasing density gradient drive (κ) shifts R vs. $\nabla\langle PV\rangle$ to the right
- Increasing frictional damping (μ) significantly reduces Zonal Flow Energy

Next Steps

- Analyze staircase and compare to zonal shear
  - See if higher local values match with higher shear flow
- Analyze correlation between $\nabla\langle PV\rangle$ and its components
  - $\nabla\langle PV\rangle$ vs. $\nabla\langle n\rangle$ and $\nabla\langle PV\rangle$ vs. $\nabla(\langle\nabla^2\phi\rangle)$

References I

[1] Akira Hasegawa and Masahiro Wakatani, "Self-Organization of Electrostatic Turbulence in a Cylindrical Plasma", Physical Review Letters, 59 (14), 1987.

[2] Balmforth, N. J., and P. J. Morrison. "A necessary and sufficient instability condition for inviscid shear flow." Studies in Applied Mathematics 102.3 (1999): 309-344.

[3] Diamond, P., Liang, Y.M., Carreras, B., & Terry, P. (1994). Self-Regulating Shear Flow Turbulence: A Paradigm for the L to H Transition. Phys. Rev. Lett., 72, 2565–2568.

[4] Fujisawa, A. (2008). A review of zonal flow experiments. Nuclear Fusion, 49, 013001.

[5] G. Dif-Pradalier, G. Hornung, X. Garbet, Ph. Ghendrih, V. Grandgirard, G. Latu, & Y. Sarazin (2017). The E x B staircase of magnetised plasmas. Nuclear Fusion, 57(6), 066026.

[6] Gurcan, O., & Diamond, P. (2015). Zonal flows and pattern formation. Journal of Physics A, 48(29), 293001.

References II

[7] J. W. S. Rayleigh. On the stability or instability of certain fluid motions, Proc. Lond. Math. Soc. 9: 57–70 (1880).

[8] H.-L. Kuo, J. Meteor. 6, 105 (1949).

[9] Numata, R., Ball, R., & Dewar, R. (2007). Bifurcation in electrostatic resistive drift wave turbulence. Physics of Plasmas, 14(10), 102312.

[10] Schmitz, L., Zeng, L., Rhodes, T., Hillesheim, J., Peebles, W., Groebner, R., Burrell, K., McKee, G., Yan, Z., Tynan, G., Diamond, P., Boedo, J., Doyle, E., Grierson, B., Chrystal, C., Austin, M., Solomon, W., & Wang, G. (2014). The role of zonal flows and predator–prey oscillations in triggering the formation of edge and core transport barriers. Nuclear Fusion, 54(7).

[11] Zhu, H., Zhou, Y., & Dodin, I. (2018). On the Rayleigh–Kuo criterion for the tertiary instability of zonal flows. Physics of Plasmas, 25(8), 082121.